Received: 12 February 2020 | Revised: 21 April 2020 | Accepted: 21 April 2020

DOI: 10.1002/pen.25408

ARTICLE

POLYMER ENGINEERING AND SCIENCE WILEY

Adhesion between thermoplastic elastomers and polyamide-12 with different glass fiber fractions in two-component injection molding

Anna-Maria M. R. Persson[1,2] | **Einar L. Hinrichsen**[1] | **Erik Andreassen**[1]

[1]Polymer and Composite Materials Group, SINTEF Industry, Oslo, Norway

[2]Department of Manufacturing and Civil Engineering, NTNU, Gjøvik, Norway

Correspondence
Anna-Maria M. R. Persson, Polymer and Composite Materials Group, SINTEF Industry, PO Box 124 Blindern, NO-0314 Oslo, Norway.
Email: anna-maria.persson@sintef.no

Funding information
Norges Forskningsråd, Grant/Award Number: 237900

Abstract

The usage of thermoplastic elastomers (TPEs) is increasing, and integrated hard-soft parts can be mass produced by two-component injection molding (or sequential molding). A key property of such parts, the adhesion between the two materials, is the topic of this study. The hard part (the first molded component) in this study was polyamide-12 with 0 to 50 wt% glass fibers (PA12-GF). As the second component, two TPEs were used: a vulcanized TPE and a styrenic TPE, both modified for adhesion to polyamides. The adhesion, assessed by 90° peel tests, increased with increasing melt temperatures and TPE injection rate, while it decreased with increasing glass fiber fraction in the PA12-GF. Based on characterization of cross-sections and fiber distributions near the interface, we propose some hypotheses for the effect of fiber fraction on the fusion between PA12-GF and TPE. These hypotheses involve the near-surface properties of the PA12-GF materials, microstructure, thermo-mechanical properties, and thermal properties. A direct effect of increasing the glass fiber fraction, that is, a reduction in adhesion as more fibers are present at the interface, does not seem to be a major effect, since few fibers are in direct contact with the TPE for any fiber fraction.

KEYWORDS

adhesion, elastomers, fibers, injection molding, interfaces

1 | INTRODUCTION

Two-component injection molding (2CIM) is a sequential injection molding process, combining two materials into one molded part. The two materials may be a soft-hard pair as in this study. An automated 2CIM process requires an injection molding machine with two injection units, and a special mold which sequentially defines the cavities of the first and second component.[1] Benefits associated with 2CIM are production efficiency and good and repeatable adhesion between soft and hard parts.[2]

Thermoplastic elastomers (TPEs) are used in an increasing number of applications, including in the automotive sector.[2,3] This study focuses on two common TPE types: styrenic TPE (TPS) and dynamically vulcanized TPE (TPV). A TPS is typically based on a triblock copolymer of styrene and a diene, in which the two hard end blocks are polystyrene, and the soft middle block is a

polydiene.[4,5] A TPV is an immiscible blend of a thermoplastic (the continuous phase) and a crosslinked elastomer.[2,4,5] Although the research toward more capable TPV types is intense,[6-8] most commercial TPV grades have a polypropylene (PP) matrix. TPV and TPS materials have different morphologies, but both have a complex phase-separated morphology.[2] A third group of TPE materials, relevant for overmolding on polyamides, is polyamide TPE (TPA). TPA materials are block copolymers with alternating hard and soft blocks, with a polyamide in the hard blocks and a polyester and/or a polyether in the soft blocks.[5] TPA materials based on various polyamide hard blocks have been reported,[9] and poly(ether-block-amide) elastomers (PEBA) based on polyamide-12 (PA12) are commercially available.

The mechanisms of adhesion relevant for polymer materials can be categorized according to its source: mechanical, molecular, and chemical. Mechanical adhesion is related to the topography of the interface; features at the micro- or macroscale hinder interfacial separation. Molecular adhesion is defined as the adhesion due to diffusion of molecules, so that molecules from one or both materials infiltrate the other. In 2CIM, this means diffusion of chain segments from one material into the other, as well as interentanglement and possibly intercrystallization. Chemical adhesion could be noncovalent chemical bonds (always present to some degree) or covalent bonds. Noncovalent bonds such as polar interactions and hydrogen bonds could be facilitated in the case of 2CIM by adding compatibilizers or by modifying the chemistry of one of the polymers by functionalization. Covalent bonds form if chemical reactions occur between the materials, and chemical reactions may occur during the molding process or in a postprocessing curing step.[10] One of the materials in 2CIM, for example, the TPE, can also be modified to have reactive groups, for example, a styrene-(ethylene-butylene)-styrene triblock copolymer (SEBS) grafted with maleic anhydride (MAH). Grafting MAH to a TPE is a common industrial method to produce a TPE with increased compatibility vs various polymers or fillers.[2,11] MAH-containing polymers can react with polyamides directly via amine end groups, and indirectly via hydrolysis of amide groups.[12]

Studies of adhesion in 2CIM have used different test geometries, see Figure 1. In studies with a butt joint (Figure 1A),[13-18] the melt flow of the soft material reaches the end of its flow path perpendicular to a surface of the hard part. Other studies employ sample geometries where the flow direction of the soft material is parallel to the side surface of the hard part (Figure 1B).[19,20] A third geometry type has the soft melt flow parallel the top surface of the hard part (Figure 1C).[21-27] The latter geometry type is used in the VDI guideline for adhesion testing of 2CIM materials.[28] These geometry types differ in terms of fusion conditions near the interface (temperature, flow, pressure) and in terms of expected uniformity of the adhesion strength. However, effects of molding conditions may be more important than flow geometry effects for the adhesion.

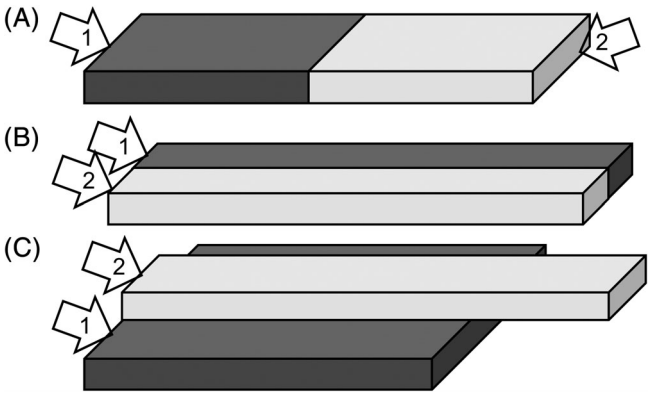

FIGURE 1 Schematics of specimen geometries. In these drawings, the first shot (hard) is dark gray and the second shot (soft) is light gray. The arrows indicate typical gate locations. A, Butt joint; B, Side surface joint; C, Top surface joint. Type C was used in this study, but with equal widths of first and second shot

Many studies of adhesion in 2CIM have used PP as the hard substrate, overmolded with TPE materials or compounds, such as TPS,[13,14] TPV,[20] and various copolymers.[22,24,25] These studies are in consensus that mold and melt temperatures are important for good adhesion, as these temperatures control the interface temperature, which in turn enables interdiffusion, and possibly cocrystallization. The TPEs in refs. [20, 22, 24, 25] had segments of either propylene, octene, or butene and, hence, a chemistry partly compatible with a hard PP substrate. However if the material pair was less compatible, the adhesion was due to interdiffusion or Rouse type fingering[24] rather than cocrystallization and could be obtained also without melting of the hard substrate.

Effects of adhesion promotors and chemical modifications have also been studied. Bräuer et al. studied 2CIM with urethane TPE (TPU) on polyamide-6 (PA6).[17,29] Introducing a chemical modifier, 4,4′-diphenylmethane diisocyanate, to the TPU, improved the adhesion, by enabling a chemical reaction between chemical groups in the soft and hard materials.[17,29] Injection molding parameters were less influential than the chemical modification, but adhesion was affected by the melt temperatures. The adhesion decreased with increasing (first shot) PA6 temperature for both modified and unmodified TPU (reduced molecular weight of the PA6 with increasing PA6 melt temperature was suggested as a cause), while the adhesion increased with increasing (second shot)

TPU temperature for modified TPU (for unmodified TPU, there was no significant effect).[17]

Hard-hard combinations have also been studied. A 2CIM study with PA66 on PA66[16] focused on the effect of mold temperature on morphology and interface strength. The adhesive strength increased with mold temperature and this was attributed to improved interdiffusion. Mold and melt temperature in combination with variothermal processing was used to control the morphology in the first component, but the morphology did not have a significant effect on the adhesive strength.[16] In a 2CIM study of PA6 on PE, which was blended with 0 to 100 wt% PE grafted with maleic anhydride (PE-g-MAH),[27] the adhesion increased with increasing PE-g-MAH fraction (the strength was almost zero without PE-g-MAH). Postmolding annealing lead to an increase in the adhesive strength (but only for PE with PE-g-MAH).[27]

There are few publications on 2CIM with glass-filled substrates. Some have reported small effects of glass fibers in the substrate on the peel force (at least for fiber fractions up to 30 wt%), while other have observed a strong negative effect. Bastian et al.[30] investigated the peel strength of TPV grades overmolded on PA6 and PA66, with and without 30% glass fibers. The TPV grades were modified for adhesion to polyamide, and had shore A values 55, 70, and 85. Good adhesion was reported for all the polyamide substrates. A figure for one of the TPVs showed that it broke in peel tests with both PA66 and PA66-GF30 substrates, and the force level corresponded to excellent adhesion. However, Bastian et al. pointed out that glass fiber contents above 30% would affect the adhesion negatively, by reducing the polyamide content at the surface, and promoting glass fiber agglomerations. Neuer[31] measured the peel force of an adhesion modified TPS overmolded on six different PA6 materials; a standard grade without any special additives, a PA6-GF30 grade, and grades with nucleating agent, impact modification, higher viscosity, green pigment or flame retardant, respectively. Among these six PA6 materials, the PA6-GF30 grade gave by far the lowest peel force; about a third of the value obtained with the standard PA6 (and even larger reduction for some molding conditions). The flame retardant also had a clear negative effect on the peel force. Islam et al.[15] studied several factors affecting the adhesion of hard-hard combinations in butt joint specimens produced by overmolding a "cold" first component, that is, not in an automated 2CIM cycle with two injection units and a special mold as described at the beginning of this section. Polystyrene (with 0 or 30 wt% glass fibers) was overmolded by either polycarbonate or a blend of polyphenylene-ether and polystyrene. The tensile tests of the butt joint specimens showed no difference between substrates with 0 and 30 wt% glass fibers for the latter material combination, and only a small negative effect of glass fibers for the former material combination (a 10% reduction, but hardly statistically significant).

The focus of the present study is the influence of the glass fiber fraction in the hard material (PA12) on the adhesion between hard and soft materials in 2CIM. The soft materials in this study (a TPS and a TPV) are modified for improved adhesion to polyamides. Note that PA12 has fewer amide groups than the more common polyamide materials PA6 and PA66.

2 | EXPERIMENTAL

2.1 | Materials

Two TPE materials where acquired from Kraiburg (Waldkraiburg, Germany): a TPV and a TPS (commercial names TV6VAZ and TC6PCZ). The TPV was based on a cross-linked SEBS (xSEBS) in a PP matrix. The TPS was also based on SEBS. Both materials were black, had a shore A hardness of 57 and were modified (by the manufacturer) for improved adhesion to polyamides.

Four commercial PA12-based materials with 0 to 50 wt % short glass fibers were acquired from EMS-Grivory (Domat/Ems, Switzerland), see Table 1. PA12 materials offer a good combination of stiffness, impact strength, chemical resistance, and geometrical tolerance.[32] The producer has published values for the storage shear moduli as function of temperature, see Appendix A1.[33] These injection molding materials have similar medium viscosity according to the datasheets; with viscosity number[34] in the range 170 to 200 mL/g (note that the viscosity number is a measure of the PA12 fraction only, the fibers do not contribute to the viscosity number).

2.2 | Injection molding trials and geometry of test specimen

The two-component test specimens were produced in an injection molding machine with 110 t clamping force (Engel ES 330H80W/110HL 2F), equipped with two injection units and a rotary table. The larger injection unit (30 mm diameter screw) was used for the hard material, and the smaller unit (22 mm diameter screw) was used for the TPE. The mold was based on the rotary plate principle. One side of the mold rotated 180° around a horizontal axis perpendicular to the parting plane, thereby defining a cavity for the second material to be injected, while also injecting one first component.

TABLE 1 PA12-based materials (manufactured by EMS-Grivory) used in the study, all heat- and UV-stabilized, and measured viscosity number (VN), glass transition temperature (T_g) and melting temperature (T_m)

Grade	ISO code	Color	VN (mL/g)	T_g, T_m[b] (°C)	E, 23°C[a] (MPa)	Density (g cm^{-3})
L 20H	PA12	Natural	154 ± 2	40, 176	1100	1.01
LV-15H	PA12-GF15	Natural			3000	1.12
LV-15H	PA12-GF30	Blue			6000	1.22
LV-15H	PA12-GF50	Black	146 ± 1	43, 177	11 500	1.47

Note: Tensile modulus (E) and density as specified by the producer.
Abbreviation: PA12, polyamide-12.
[a]Conditioned.
[b]Measured by differential scanning calorimetry.

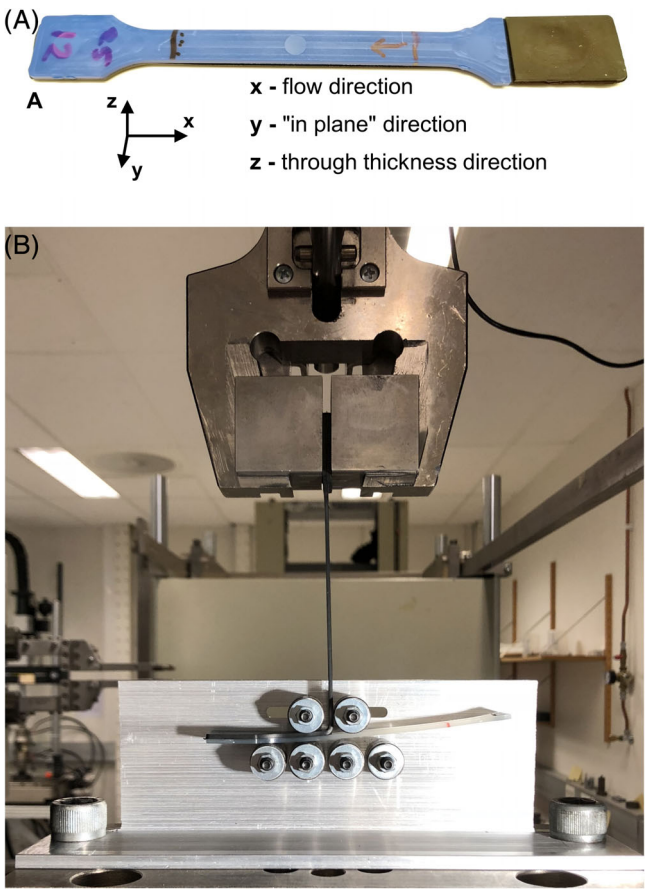

FIGURE 2 A, A representative peel specimen, prior to testing, here made of PA12-GF30 (blue) and a black TPE (covering the entire bottom part of the specimen). Markings on the polyamide surface: The lines define the beginning and end of the peeling, and the arrow shows the direction of the peel. The TPE component was cut free from the hard component, from the right hand side to the line with the arrow. B, The experimental setup for the 90° peel test. Here with a test specimen of natural PA12 and black TPE. PA12, polyamide-12; TPE, thermoplastic elastomer [Color figure can be viewed at wileyonlinelibrary.com]

A 2CIM specimen is shown in Figure 2A. It is based on a standard tensile test specimen; type 1A of ISO 527-2. Except the TPE peel tab, the polyamide and TPE parts were both 2 mm thick. The mold surface corresponding to the surface of the hard part to be overmolded was prepared by blasting with glass particles in order to achieve a surface roughness with Ra 4.5 μm. This roughness value conforms with the range given in a guideline.[28] Compared to the original milled surface, this roughening gave a large increase in adhesion.

The melt temperatures of the hard and soft materials, and the injection time for the soft material, were varied in this study. The studied combinations of materials and melt temperatures are shown in Table *2*. The other processing parameters were kept fixed, based on recommendations from the suppliers, and judgment of good parts.

2.3 | Adhesion test (90° peel test)

Before testing, the specimens were stored at 22°C to 23°C for minimum 4 weeks, and then conditioned minimum 24 hours at 23°C and 50% relative humidity. The tests were performed at 23°C. The adhesion between the TPE and the polyamide-12 with 0 to 50 wt% glass fibers (PA12-GF) was measured in a 90° peel test, using a universal testing machine (Zwick/Roell Z250), with a 2.5 kN load cell, see Figure 2. The width of the peeled layer was 10 mm, that is, the full width of both molded parts in the narrow section of the test specimen. Prior to the test, a lip of the TPE was cut free with a sharp carpet knife, to a distance of 10 mm, see Figure 2A. The test specimen was kept in position by a fixture with rollers as shown in Figure 2B. The crosshead speed was 50 mm/min and the peel length was 70 mm. In some tests, the horizontal displacement was logged separately. This reduced the peel length to about 50 mm. First, it was checked if the force vs distance curve had a pronounced initialization peak. An average peel force, F_{peel}, was calculated from each peel test, based on an identified plateau zone of the force vs displacement data. The F_{peel} calculation excluded the initial peak force and also artifacts at the end of the

TABLE 2 Combinations of used materials and melt temperatures (T_{soft} and T_{hard})

Soft material	T_{soft} (°C)	Hard material	T_{hard} (°C)
TPV	210, 230, 250, 270	PA12	255
TPV	250, 270	PA12-GF15	255
TPV	250, 270	PA12-GF30	255, 285
TPV	250, 270	PA12-GF50	255, 285
TPS	230, 250	PA12	255
TPS	230, 250, 270	PA12-GF30	285

Note: Moreover, the filling time for the TPE was varied (0.8, 1.6, and 3.0 seconds) for most melt temperature combinations. The filling time for the hard part was constant at 0.5 second. The mold temperature was measured to 40°C.
Abbreviations: TPE, thermoplastic elastomer; TPS, styrenic thermoplastic elastomer; TPV, vulcanized thermoplastic elastomer.

peeling. Hence, F_{peel} is the force corresponding to stable peeling. The tests in which the horizontal displacement was measured confirmed that the force plateau corresponded to peeling progressing over the specimen length.

2.4 | Characterization of materials and surfaces

A Fourier transform infrared spectrometer, Cary 670 series from Agilent Technologies, was employed to characterize the chemical composition of the injection molded parts. The infrared (IR) absorption spectra were measured in attenuated total reflection (ATR) mode, with a diamond crystal having an analysis depth of approximately 1.7 μm for polymers at 1000 cm^{-1}. The surface (as molded) and bulk (fresh cuts) of injection molded PA12-GF parts were characterized, as well as the surface of the TPE parts. To evaluate the concentration of fibers near the surface of PA12-GF50, the spectrum of this surface was compared to those of the (neat) PA12 surface and the bulk of PA12-GF50, for the broad absorption assigned to glass from about 1300 to 810 cm^{-1}.

The viscosity number[34] of some of the PA12 materials (pellets) was measured with m-cresol as solvent. The method was based on ISO 307,[34] except that a rotational rheometer was used (Physica MCR300 rheometer, employing a 50 mm cone and plate fixture). For various polyamides, this modified method has shown to give results similar to ref. [34].

White light interferometry (WLI), with a Wyko NT9800 instrument, was employed to characterize the surface topography of the hard parts (which were not overmolded), in the center of the surface intended for overmolding. The topography of the surface allowed for measuring 68% of the area with this instrument and the chosen optics. The measurements were repeated twice on areas sized 0.30 × 0.40 mm (pixel size 0.36 μm). WLI was also employed to characterize the laser engraved lines, with a measurement area of 1.10 × 0.86 mm (pixel size 1.8 μm). The measurements were analyzed with software from Wyko and Gwyddion.

Cross-sections of 2CIM parts and polyamide parts (not overmolded) were cast in transparent epoxy and polished. The cross-sections were cut in the y-z plane (Figure 2A), halfway along the flow path (x direction). Hence, in the microscope pictures of cross-sections, the hard-soft interface is horizontal (but not a straight line), with the hard and soft components above and below the interface, respectively. The cross-sections were characterized by optical microscopy. Optical microscopy was also used to inspect the laser engraved lines. Scanning electron microscopy (SEM) of the cross-sections was performed with low vacuum, and high vacuum after gold plating.

Hot stage microscopy was performed with a Linkam THMS350V, using a heating rate of 10°C/min up to 205°C. The samples were 10 to 20 μm thick flakes of PA12 and PA12-GF30, cut off with a scalpel from the skin layer of injection molded specimens.

A laser engraver (LaserPro Spirit GX), with a CO_2 laser (wavelength around 10 μm, ie, mid-IR radiation), was used to engrave shallow lines on PA12-GF specimens—on the surface overmolded in the 2CIM trials, corresponding to the milled mold surface. The idea behind this experiment was to analyze the melting of the surface, for materials with different glass fiber contents. Three different laser power levels were used. The laser path was perpendicular to the flow direction.

3 | RESULTS

3.1 | 90° peel tests—Effects of glass fiber content and process conditions

Results from peel tests of specimens overmolded with the TPV are shown in Figure 3A to D, and the main trends can be summarized as follows: The adhesion (peel force)

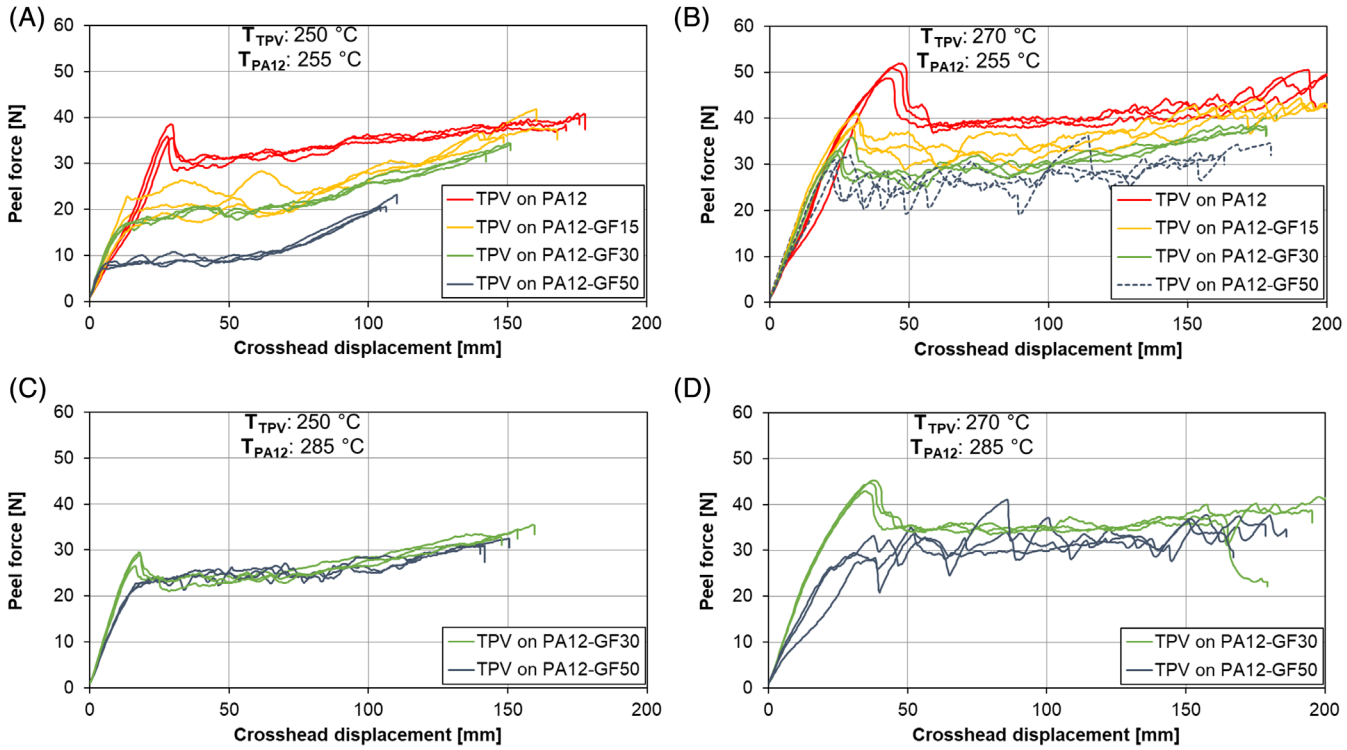

FIGURE 3 Peel force vs crosshead displacement for TPV on PA12 with 0 to 50 wt% GF. The melt temperatures of the materials are given in each figure. The TPE filling time was 1.6 seconds in all cases, except in (B) (0.8 second; dashed curve). Curves for three repeated tests are shown in each series. PA12, polyamide-12; TPE, thermoplastic elastomer; TPV, vulcanized thermoplastic elastomer [Color figure can be viewed at wileyonlinelibrary.com]

increases with decreasing glass fiber content in the hard material. However, for some processing conditions, as in Figure 3C, the effect is small; in this figure, the fiber content mainly influences the initial peak force. Comparing Figure 3A with Figure 3B shows that increasing the TPV melt temperature (from 250°C to 270°C) increases the adhesion. The same trend is seen when comparing Figure 3C with Figure 3D. Comparing Figure 3A with Figure 3C shows that increasing the melt temperature of the (first injected) hard material (from 255°C to 285°C) also increases the adhesion, in particular for PA12-GF50. The same trend is seen when comparing Figure 3B with Figure 3D. The fill time for the TPV also has some effect on the adhesion as seen in Figure 4. Reducing the fill time from 1.6 to 0.8 second increases the adhesion, but there is no significant difference between the fill times 1.6 and 3.0 seconds, with this set of molding parameters.

To put the peel force values in perspective, the VDI guideline[28] ranks adhesion levels based on the peel force per specimen width. A value above 2.5 N/mm is characterized as "very good," and a value above 4 N/mm as "excellent." In our case, the specimen width (hard and soft part) is 10 mm. Note that in the VDI guideline, the hard substrate is wider than the soft specimen, which gives a more uniform adhesion over the specimen width.

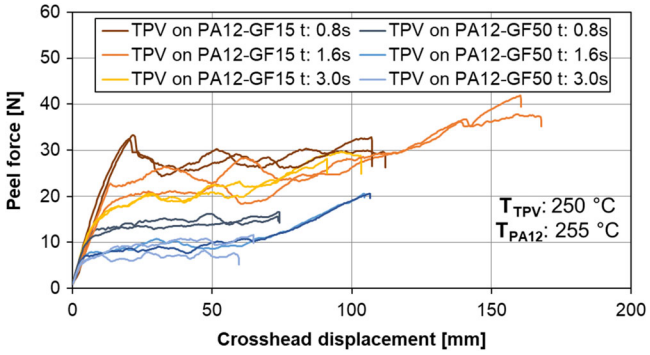

FIGURE 4 The influence of injection time of the TPV (0.8, 1.6, and 3.0 seconds) on peel force. Results for TPV on PA12-GF15 and PA12-GF50. Curves for two specimens are shown for each series (curves with the same color). TPV, vulcanized thermoplastic elastomer [Color figure can be viewed at wileyonlinelibrary.com]

The TPS (Figure 5) generally showed higher peel forces than the TPV (Figure 3), and in the best cases the adhesion was so high that the stretched TPS part broke while initiating the peeling (at a force corresponding to a nominal tensile stress around 3 MPa). The TPS showed the same trends as the TPV regarding peel force vs glass fiber content and melt temperature (Figure 5).

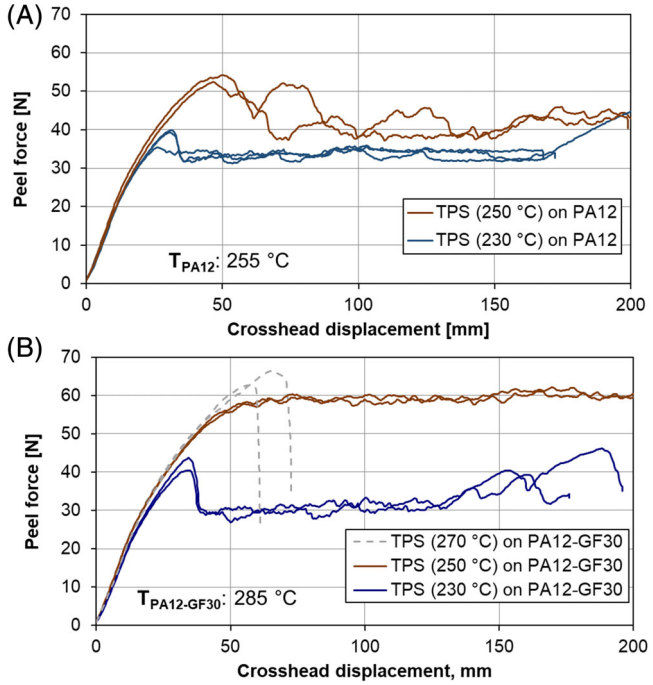

FIGURE 5 Peel force vs crosshead displacement for TPS on, A, PA12 and, B, PA12-GF30. The respective melt temperatures are shown in the diagrams, and the injection time was 1.6 seconds. The dashed series in (B) corresponds to tensile failure of the TPE. PA12, polyamide-12; TPE, thermoplastic elastomer; TPS, styrenic thermoplastic elastomer [Color figure can be viewed at wileyonlinelibrary.com]

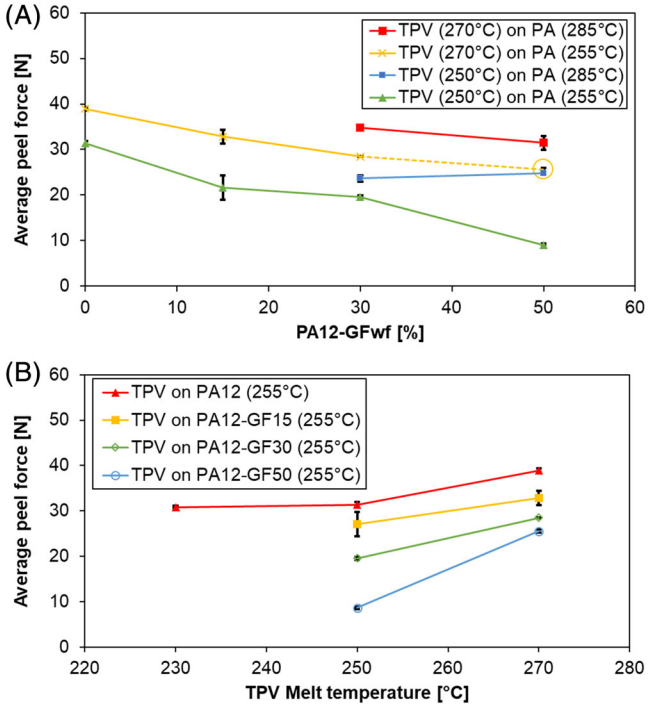

FIGURE 6 Average peel force for the TPV vs, A, glass fiber fraction of the PA12 and, B, melt temperature of the TPV. The temperatures in the legends are the melt temperatures of the respective materials. The injection time of all TPVs was 1.6 seconds except for 0.8 second in (A) yellow data point connected to a dashed curve. PA12, polyamide-12; TPV, vulcanized thermoplastic elastomer [Color figure can be viewed at wileyonlinelibrary.com]

Referring to the force-displacement curves in Figure 3, some observations can be noted. Up until a peak force or at a marked change in the slope, the recorded crosshead displacement only corresponds to elongation of the TPE part. This was confirmed by peel tests in which the peeling distance was measured in addition to the crosshead displacement. Note that an initial peak force, corresponding to peeling initialization, was not observed for cases with low adhesion, and it was not observed for any of the specimens based on PA12-GF50. After initialization of peel, the force reaches a plateau, corresponding to a steadily advancing peel. In some cases, this plateau has a small positive slope. Comparing the force curves during peel in Figure 3A with Figure 3B, it seems that sloping peel curves occur when the adhesion is low, while rather flat plateaus are seen when the adhesion is higher. Toward the end of the test, in some cases, the curves show a marked increase in force. This is an artifact as a result of the arrest of the peel when reaching the end of the narrow section of the test specimen.

An average peel force, F_{peel}, was calculated for each peel test as described in the Section 2. Trends for this average peel force for the TPV are shown in Figure 6, highlighting quantitative effects of glass fiber content and process parameters.

3.2 | Microscopy of peeled surfaces

Microscopy of the hard surface after peeling is shown in Figure 7. The amount of TPE residue increases with increasing TPE melt temperature, and there are also some picture pairs (Figure 7A,E, and Figure 7B,F) that show that the amount of residue decreases with increasing glass fiber content. The TPE residue content is generally higher in the central zone of the specimen width. The Figure 7D shows an exception, where there are three zones over the width of the specimen (vertically in the picture): At the center, there is medium residue content at most of the width, then a narrow band with high content, and finally an outer band of about 1 mm without residue. Compared to the TPV, the TPS shows a higher and more uniform residue content (better adhesion). Figure 7E (TPV on PA12-GF30, with poor processing conditions) shows a case with no visible residues.

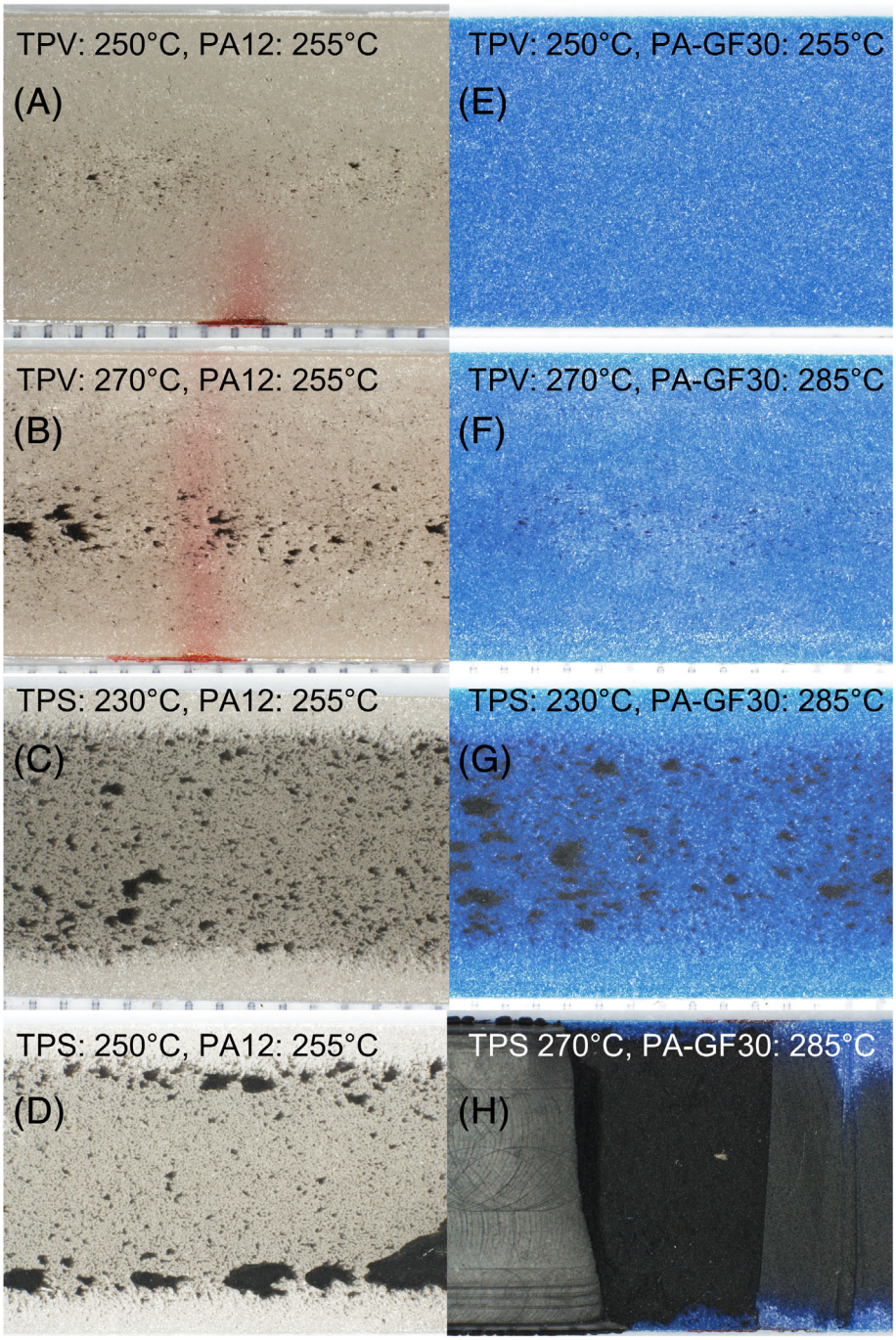

FIGURE 7 Microscopy of the hard substrate after the peel test (peel direction right to left). The depicted areas are positioned 20 mm into the peel, and the full width (10 mm) of the specimens is shown. Black spots are residues of TPE on the hard substrate. The melt temperatures are given in each micrograph. TPE, thermoplastic elastomer [Color figure can be viewed at wileyonlinelibrary.com]

3.3 | IR spectroscopy of as-molded hard polymer surfaces and TPE materials

The IR spectra measured on the as-molded surfaces of the hard materials show virtually no differences between PA12 and PA12-GF (15-50 wt% GF). The peaks agree with those in PA12 literature.[32] Comparing the surface and bulk spectra, Figure 8A shows that the surface spectrum of the PA12-GF50 is closer to the spectrum of the (unreinforced) PA12 than the bulk spectrum of the PA12-GF50. Considering the broad glass band around 945 cm^{-1}, the IR spectra show that, for the PA12-GF50, the glass content is clearly lower at the surface than in the bulk. A numerical analysis of the spectra of the surface of PA12, the bulk of PA12-GF50 and the surface of PA12-GF50, showed that combining 8% of the PA12-GF50 bulk spectrum and 92% of the PA12 surface spectrum gave the best fit to the PA12-GF50 surface spectrum. Consequently, the fraction of glass fibers at/near the surface (ie, within the ATR analysis depth of about 1-2 μm) is estimated to be 4 ± 3 wt% (95% confidence, $N = 2$), under the assumption that the glass fraction in

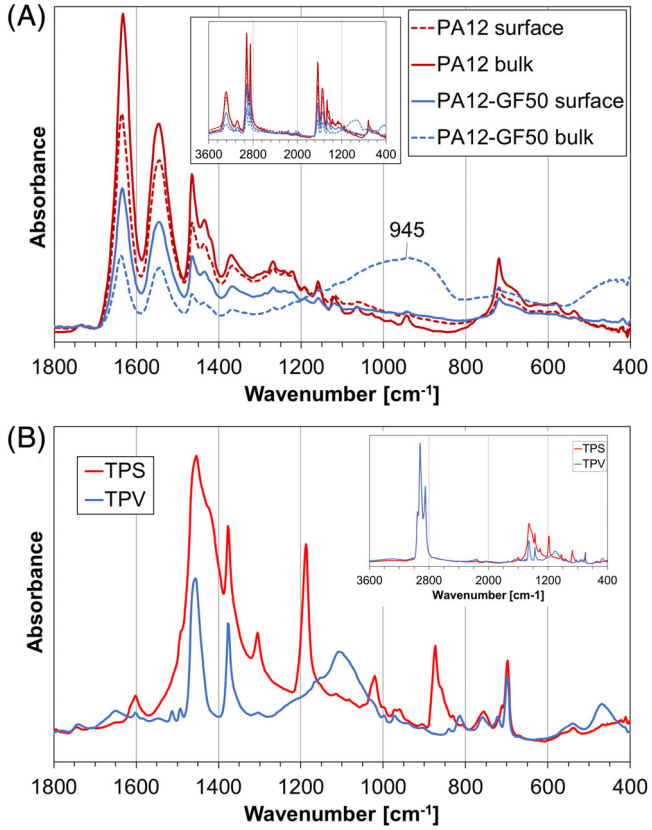

FIGURE 8 IR spectra of, A, PA12 and PA12-GF50, and, B, TPE (surface). IR, infrared; PA12, polyamide-12; TPE, thermoplastic elastomer [Color figure can be viewed at wileyonlinelibrary.com]

the bulk of PA12-GF50 is 50 wt%, since the core layer is much thicker than other layers.

The IR spectrum of the TPS (in Figure 8B) shows bands related to styrene blocks and the aromatic ring[32,35] and others related to the ethylene-butadiene blocks of SEBS.[36] The TPS has bands at 1601 and 1493 cm^{-1} that coincide with bands observed for a commercial SEBS-g-MAH,[11] but the expected band at 1709 cm^{-1} is weak. As elaborated in ref. [37], bands associated with SEBS-g-MAH would overlap with bands associated with the aromatic ring. The TPS is likely hydrogenated, as there is no peak at 1645 cm^{-1} to associate with a double bond between carbons. The TPS also shows bands at 1188 and 874 cm^{-1} which are not related to pure SEBS.

The TPV spectrum has bands related to styrene, that coincide with bands in ref. [11]. There is also a weak band at 1645 cm^{-1} associated with the double bond of butadiene.[36] Ref. [38] used the intensity of a band at 1780 cm^{-1} as an indicator of MAH grafting of in-house produced grafting, but this band was weak (TPV) to invisible (TPS) in our spectra (Figure 8B). Note that in ref. [37], this band could only by deduced by decomposing the spectra, but in ref. [11] this band was not visible.

3.4 | Roughness of as-molded hard polymer surfaces

WLI of the hard polymer surfaces (specimens not overmolded) gave a mean roughness (Ra) of 4.8 ± 0.3 μm and a root-mean-square roughness of 6.1 ± 0.4 μm. There was no significant effect of glass fiber content on the measured roughness.

3.5 | Optical microscopy of hard-soft cross-sections

Figure 9 shows microscopy images of polished cross-sections of PA12 and PA12-GF overmolded with TPV, as well as not overmolded parts. The nature of a 2D section reduces the interface between the materials down to a line. Figure 9A,E shows PA12 overmolded with TPV at 250°C and 270°C, respectively, indicating that a higher TPV temperature gives a smoother interface. This effect can also be seen with PA12-GF15 (Figure 9B,F). However, for PA12-GF30 (Figure 9C,G) and PA12-GF50 (Figure 9D,H), the effect of TPV temperature is less pronounced. Figure 9I to L shows the surface topographies of the as-molded hard materials, and the roughnesses are similar for all glass fiber contents. For the PA12, the overmolding had a smoothening effect (Figure 9I,E) while the PA12-GF50 was relatively unaffected by overmolding (Figure 9H,L). Appendix B1 shows the uncropped versions of the micrographs in Figure 9.

3.6 | SEM of hard-soft cross-sections

The SEM micrographs in Figure 10 show that, regardless of fiber content, very few fibers are in contact with the TPE surface. On the hard side of the interface, a layer of 20 to 50 μm had a lower fiber concentration than the bulk. The minimum distance between the TPE surface and a glass fiber appeared to be about 10 μm.

As in Figure 9, the SEM micrographs in Figure 11 illustrate how the overmolding may smoothen the surface topography of the hard surface. Hard surfaces before overmolding are shown in Figure 11A,B, and overmolded surfaces are shown in Figure 11C to F. With PA12-GF15 (and the PA12 without fibers), the hard surface was smoothened by the overmolding process, likely because the heat from the second shot softened the skin layer of the hard surface. In contrast, the PA12-GF50 surface topography was less affected by the overmolding. Higher magnifications of these SEM micrographs are available in Appendix C1.

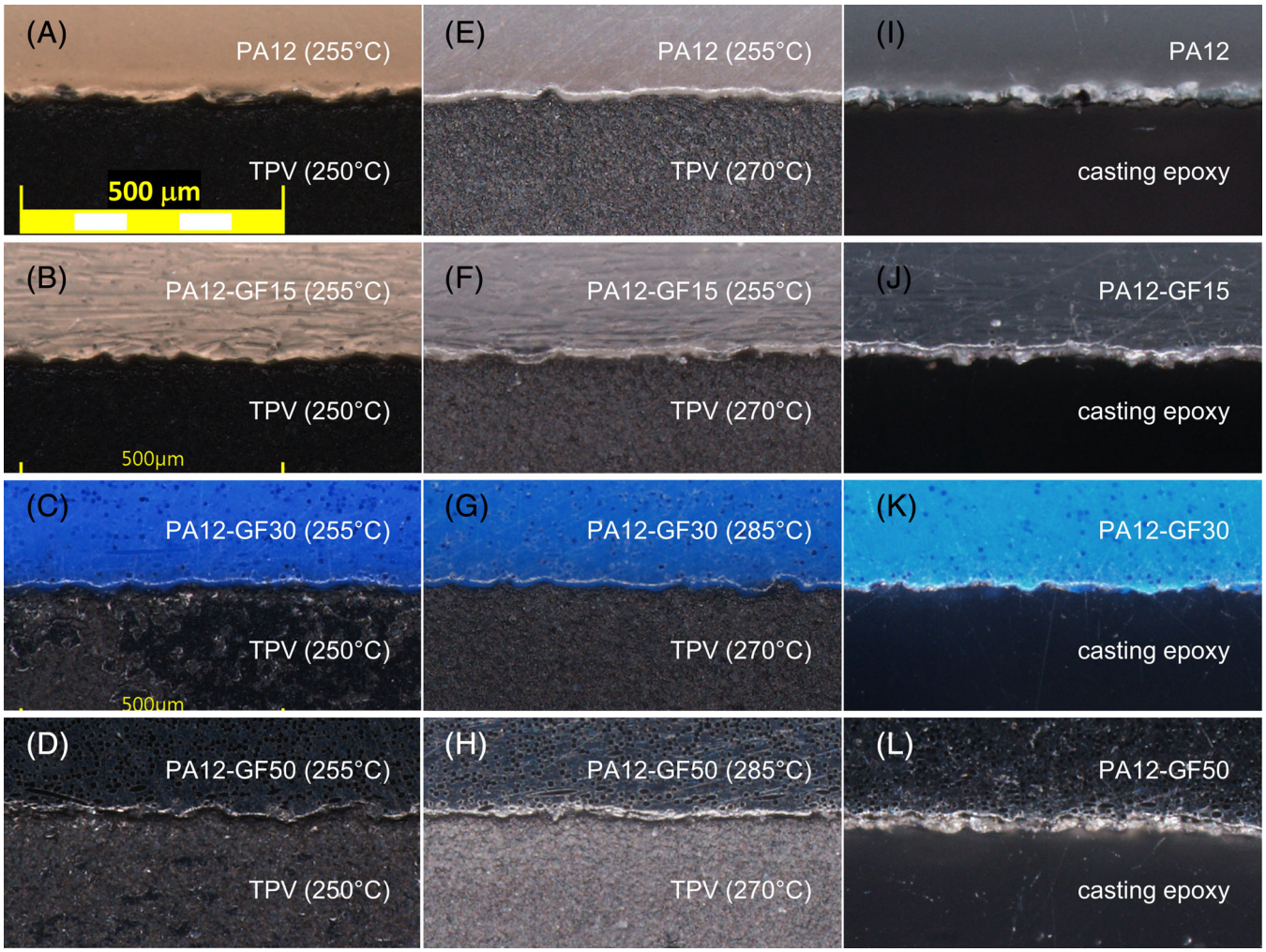

FIGURE 9 Optical microscopy of cross-sections of PA12-GF overmolded with TPV, and without overmolding (right column). The (injection molding) flow direction is into the paper plane, and the cross-section is halfway along the flow path (Figure 2A). Hence, the interface between the two materials is horizontal in the pictures. TPV, vulcanized thermoplastic elastomer [Color figure can be viewed at wileyonlinelibrary.com]

3.7 | Hot stage microscopy of PA12 vs PA12-GF30

Hot stage microscopy of approximately 10 µm thin flakes of PA12 and PA12-GF30, cut from the skin layer of IM specimens, demonstrated the difference in viscosity between the unfilled PA12 and the PA12-GF30, see Figure 12. The fibers resist the flow.

3.8 | Laser engraving of hard polymer surfaces

The laser-engraved grooves were characterized by WLI and optical microscopy. In most cases, the laser created a groove flanked by ridges. A few 2D WLI profiles are shown in Figure 13, and WLI plots are available in Appendix D1. Some characteristics of the laser-engraved grooves are shown in Table 3.

At low to intermediate laser power (P1-P2), the material volume was conserved (cross section of groove approximately equal to cross section of the ridges). At the high power level (P3), the volume was conserved for low glass content (0 and 15 wt%), while for high glass content (30-50 wt%) the volume was reduced.

With the lowest laser power (P1), 3 to 5 µm high ridges were formed for PA12 and PA12-GF15, while ridges/grooves could not be clearly identified for PA12-GF30. The roughness parameter in Table 3 was calculated along the laser path, and it indicates how unevenly the surface has deformed along the groove. At P1, it was noticed that melting took place between fibers, which remained covered with PA12 matrix. At higher power levels, more glass fibers were exposed, but still the

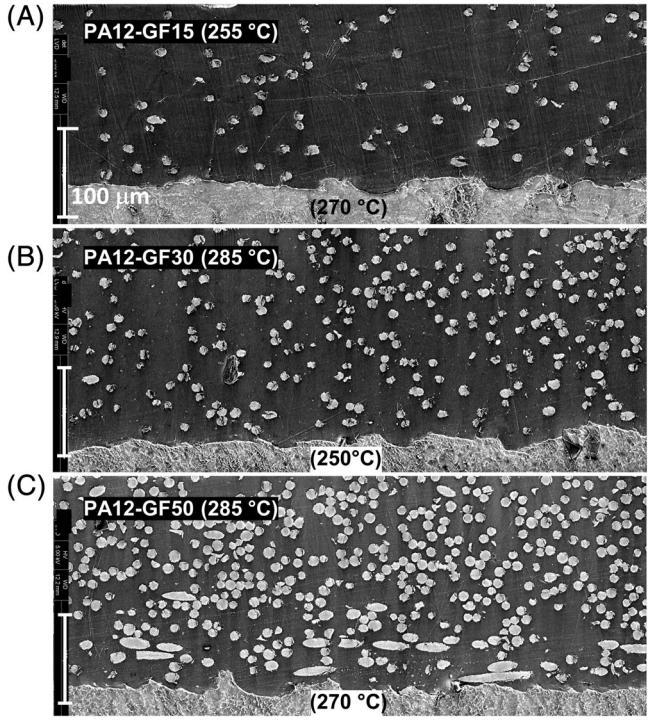

FIGURE 10 Low vacuum SEM of cross-sections, showing the distribution of fibers near the hard-soft interface (the TPE is seen at the bottom of the micrographs), for different glass fiber fractions. The cross-section is halfway along the flow path (Figure 2A). Hence, the interface between the two materials is horizontal in the micrographs. The PA12 (dark gray) with glass fibers (light gray circles or ovals) is seen above the interface, and the TPE (light gray) is below the interface. The melt temperatures of the materials are given in each micrograph. PA12, polyamide-12; SEM, scanning electron microscopy; TPE, thermoplastic elastomer

topography was lower around fibers. At power levels P2 and P3, a topography with a groove flanked by ridges was created on all substrates, and the local surface was smoothened (except for the overall shape) for unfilled PA12, see Figure 13. At power level P3, the shape of the groove was affected by the glass fibers: Compared to fiber filled substrates, the unfilled PA12 had a deeper groove, the ridges were higher, and the distance between the ridges was somewhat smaller (Figure 13).

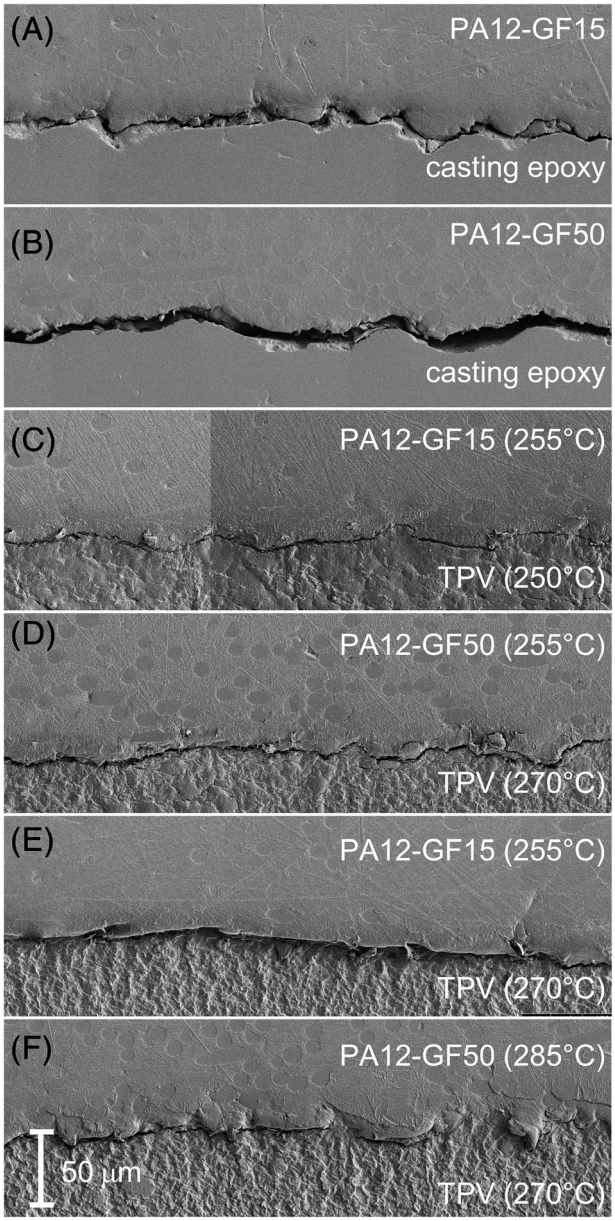

FIGURE 11 SEM of gold coated cross-sections of (A, C, E) PA12-GF15 and (B, D, F) PA12-GF50, either (A, B) without overmolding or (C-F) with TPV overmolding. The melt temperatures of the two materials are given in each micrograph. The contrast was moderately enhanced to improve the visibility of the glass fibers. SEM, scanning electron microscopy; TPV, vulcanized thermoplastic elastomer

4 | DISCUSSION

There are several factors that can affect the adhesion between the soft and hard material in 2CIM. The relative effect of these factors may vary depending on the selected 2CIM part geometry. For this study, we selected the "top surface joint" (Figure 1C), as it was considered relevant for a majority of industrial 2CIM applications.

The surface roughness of the hard part (first shot) is important; compare blasted vs milled surfaces mentioned in the Section 2. Rossa-Sierra et al.[18] and Islam et al.[15] reported that the adhesion increased with increasing surface roughness, and attributed this to better mechanical interlocking, and also more localized heating and melting. However, in our study, the surface roughness of the first shot was kept constant for all materials and processing conditions.

The standard versions of the TPEs in this study do not adhere adequately to polyamides. Hence, in this

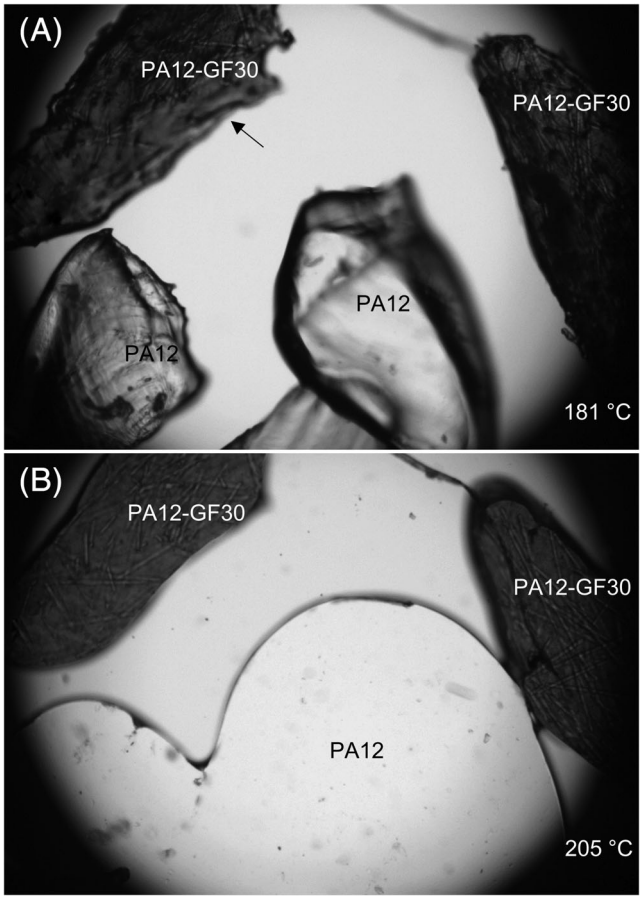

FIGURE 12 Hot stage microscopy, showing the melting and flow of PA12 and PA12-GF30. A, At 181°C, some PA12 flakes appear melted, while the PA12-GF30 flake shows signs of melting near its edge (arrow). B, At 205°C, after 150 seconds hold time, the PA12 flakes has flowed into a pool, while the PA12-GF30 flakes stay in similar shape as prior to melting. PA12, polyamide-12

study, we used TPEs which were chemically modified for adhesion to polyamides. The adhesion mechanism(s) for these modified TPEs is not published, but a chemical reaction with the polyamide may contribute to the adhesion. The IR spectra could not identify the chemical modification of these TPE materials.

A PA12-based poly(ether-block-amide) elastomer (TPA) was also included in the initial injection molding trials, with PA12 and PA12-GF30 as the hard materials. This TPA was expected to adhere to PA12, but it was excluded from the study due to demolding problems, especially at high melt temperatures.

The well-known effect of temperature on adhesion was observed. The increase in adhesion with increasing melt temperature (of either soft or hard material) agrees with most studies referred to in the Section 1. Avoiding material degradation generally sets the upper limit of melt temperatures. Arzondo et al.[22] elaborated that the interface temperature during overmolding is a function of both first and second shot melt temperatures (as well as the mold temperature). Hence, in order to achieve a high enough interface temperature, all temperature parameters and their admissible ranges are important.

The adhesion was improved with increasing TPE injection rate. Faster injection leads to a higher shear rate, which increases shear induced heating, as well as less time for cooling during injection. The heating is largest where the shear rate is highest, near the wall, that is, near the interface to the hard component. Candal et al.[20] observed the same positive effect of increasing the TPE injection rate, and interpreted this in terms of a competition between the positive effect of higher temperature (less time for the TPE to cool before contacting the

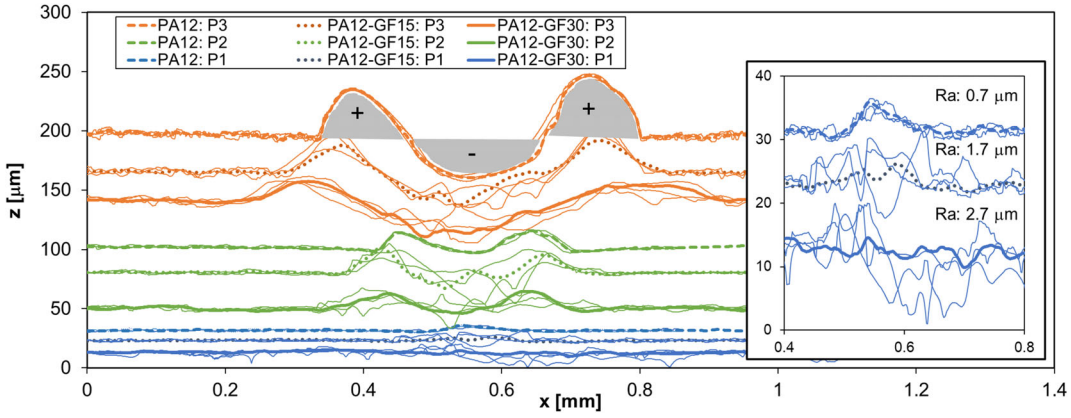

FIGURE 13 WLI profiles over the laser engraved specimens. The thin lines correspond to measurements on a 1.8 µm segment along y and the thick lines are averaged 0.18 mm segments. A combination of ridge (+) and valley (−) cross-sections (marked in gray) allows for estimating volume change of the specimens. The initial Ra values are marked in the inlay of P1 WLI profiles (blue lines). WLI, white light interferometry [Color figure can be viewed at wileyonlinelibrary.com]

TABLE 3 Characteristics of the laser-engraved grooves as measured by WLI

Laser power	GF (wt %)	Peak[a] (μm)	Ra, initial (μm)	Ra, groove[b] (μm)
P1	0	5		0.2
P1	15	3		0.7
P1	30	—		2.1
P2	0	14	0.7	0.3
P2	15	16	1.7	4.4
P2	30	15	2.7	3.7
P3	0	49		1.9
P3	15	26		5.8
P3	30	16		4.6

Note: P1 is the lowest laser power used and P3 is the highest. Note that the engraving was performed on the surface (to be overmolded) corresponding to the milled mold surface, but the initial roughness was not the same for these three samples (some from a preproduction run).

Abbreviations: GF, glass fibers; WLI, white light interferometry.

[a]Average height of ridges.

[b]Ra along laser path.

substrate) and a negative effect of higher injection pressure (possibly via residual stresses or diffusion of low molecular weight species in the TPE to the interface). Islam et al.[15] explained a similar effect of injection rate by increased shear heating and (as opposed to Candal et al.) a positive effect of higher injection pressure.

The effect of melt temperature could be a pure thermal effect (better physical fusion), but higher temperature could also favor a possible chemical reaction between adhesion modified TPE and PA12, and increase the number of chain segments from the two materials that are brought in contact. In some cases, the peel force plateau has a positive slope. The reason for this could be that the peel direction is opposite to the TPE flow direction, and the heat transfer from the TPE injection is higher near the gate, as also proposed by Bastian et al.[30]

The adhesion decreased with increasing glass fiber fraction in the PA12 (Figure 6A). A similar reduction was reported in ref. [31], while the refs. [15, 30] reported almost no effect of glass fibers. Refs. [30, 31] both studied TPEs modified for adhesion to polyamides, but these papers are sparse on details which could explain why their results are so different. The third study[15] differed from our study in several aspects (it used hard-hard material combinations and butt joint specimens), so the variable dependencies may be different.

In the following, we assume that, for the hard materials in this study, the PA12 matrix is nearly the same regardless of glass fiber content, that is, that the PA12 matrix has the same molecular mass, melting point, and so on. This is based on the measured thermal and rheological properties as shown in Table 1. With this assumption, we have some hypotheses for the observed reduction in adhesion with increasing glass fiber fraction:

1 A straightforward hypothesis could be that there is a direct effect of the glass fiber content, because the adhesion between TPE and glass is probably lower than that between TPE and PA12. Ref. [30] showed microscope images of agglomerated glass fibers on a PA6-GF50 surface, and suggested this to cause reduced adhesion strength. However, in our study, such glass fiber agglomerates at the surface were not observed, and microscopy of the hard parts showed that very few glass fibers are in direct contact with the TPE. IR spectroscopy of the PA12-GF50 indicated that the fraction of fibers on/near the surface is around 4 wt% (with an ATR analysis depth of 1-2 μm), and, hence, an even lower volume or area fraction. Therefore, a direct effect of glass fibers at the surface does not seem to be the primary explanation. A lower fiber concentration near the surface was also found in other studies: X-ray computed tomography was used to locate individual fibers in glass reinforced PA12[39] and PA6.[40] In ref. [40], with PA6-GF30, the fiber fraction was 5 vol% at a distance 0.25 mm from the surface, as compared to the nominal value of about 15 vol% (corresponding to 10 and 30 wt%).
2 Another simple hypothesis could be that the surface roughness of the molded hard part (prior to the TPE overmolding) is affected by the glass fiber content in the material. However, for our study, this hypothesis can be rejected, because WLI and SEM showed that the roughness of the hard part was similar for all glass fiber fractions.
3 A third hypothesis could be that the glass fiber content, via flow effects and/or thermal effects, affects microstructural features of the PA12 in the skin layer of the hard part, which, in turn, could affect the ability of the hard surface to fuse (including interdiffuse) with the overmolded TPE.
4 Somewhat related to hypothesis 3, a fourth hypothesis could be that the "near-surface" thermo-mechanical or rheological properties of the hard material may have an effect on the fusion mechanism and the resulting adhesion.
5 A fifth hypothesis could be that the thermal properties of the hard part depend on the glass fiber content, and that this affects the cooling of the hard part (first shot) in the mold prior to overmolding, as well as the heating of this material at the interface, as the TPE melt contacts the hard part.

For the three last hypotheses, an important question is how the local "near-surface" properties of the hard part differ from the bulk properties. Additionally, what is the relevant depth of the International Organization for Standardization 375 hard part (from the surface and in) which must be considered, in order to analyze the effect of the glass fiber fraction on the fusion mechanism? The fiber concentration near the surface influences all three hypotheses; it affects chain mobility (close to a fiber), stiffness/flowability, and thermal properties. Furthermore, is the hard surface melted by the TPE, or just heated so high above the glass transition temperature that some interdiffusion occurs, or maybe only chemical reactions occur at the interface?

According to ref. [14], the thickness of the interdiffusion zone for 2CIM could be a few micrometers. Our SEM micrographs at the highest magnification did not show any evidence of a distinct interphase (Appendix C1), but contrast methods could have revealed details of the interphase. IR microscopy of cross-sections did not give reliable high-resolution results near the interface, due to uneven surfaces meeting at the polished interface, partly caused by the mismatch in stiffnesses of the two materials.

The laser engraving experiment indicates that the glass fiber fraction may indirectly affect the adhesion, which supports hypotheses 3 to 5. The effect of the laser on the topography depended on the laser power and the glass fiber fraction. At low laser power the polymer melted, while at high power levels the polymer was partially ablated, based on the observation of either conserved volume or loss of volume. Melted polymer is believed to form the observed ridges due to surface tension. At the lowest laser power, a depth of around 5 μm was affected. This is a depth which seems to be relevant for 2CIM interdiffusion in general. The pattern left by the laser was affected by the glass content, even without exposing fibers. The fibers appear to behave as heat sinks, transferring heat away from the surface and into the bulk, resulting in a lower temperature near the surface (and the interface). The laser-induced pattern reflected the positions of individual fibers near the surface, revealing that the fibers near the surface are mainly oriented in the surface plane. This can also be seen in the SEM micrographs of cross-sections (Figure 10).

Regarding hypothesis 3, we define the skin layer as the layer which solidifies directly as the melt front fountain flow contacts the mold surface. The skin layer typically has a lower fiber fraction than the bulk material, but this hypothesis is mainly concerned with the PA12 microstructure in the skin layer (refer to the polarized micrograph of PA12 in Appendix E1). Several structural features of the PA12 in the skin layer, as well as the skin layer thickness as such, could be affected by the glass fiber content: Morphology (including crystallinity and orientation), chain length (via flow-induced segregation), or stress-induced chemical degradation. These skin layer features may affect the softening or melting of the skin layer, and, hence, the fusing ability. In addition to such PA12 microstructure effects, the PA12 chain mobility may be reduced close to glass fibers.

There are indications in the literature that the glass fiber fraction may affect the polymer microstructure in the skin layer. Ref. [39] studied the fiber orientation in injection-molded plates of PA12-GF with X-ray computed tomography. The fiber fraction (15%, 30%, and 50%) affected the fiber orientation distribution over the cross-section, as well as flow characteristics. Ref. [39] argued that increasing the fiber fraction increased the tendency for plug flow and flow irregularities (viscous fingering). This indicates that the fiber fraction may affect structural features of the skin layer. Furthermore, the skin layer microstructure and thickness will vary with processing conditions and along the flow path, as reported for PA66 in ref. [41].

Regarding hypothesis 4, the bulk stiffness and the viscosity clearly increase with increasing fiber content (Appendix A1 and Figure 12). Also, the stiffness reduction when increasing the temperature from 23°C to 150°C is higher for PA12 than for PA12-GF50 (−87% and −60%, respectively, see Appendix A1). Can this affect the fusing mechanism, and partly explain the effect of fiber content on adhesion?

A stiffer PA12-GF surface (ie, a material with a higher glass fiber fraction) may restrict the TPE flow/pressure induced deformation or erosion of the hard surface topography, either below or above the melting point. If melting of a surface layer occurs, a higher viscosity due to a higher fiber content will affect the flowability. There are indications that the TPE flow/pressure smoothens the hard surface (first shot), and the degree of smoothening depends on melt temperature and fiber content (Figures 9 and 11). This observed smoothening can also be seen as a proof of a "near-surface" effect of fiber content. (Note that, in addition to smoothening, the TPE flow may also induce irregularities [eg, ripples] on the surface of the first shot.) A smoothening may reduce the adhesion, by reducing the mechanical anchoring effect, but smoothening may also be a sign of a softening of the first shot, and then the degree of smoothening may be positively correlated with the degree of interdiffusion. Hence, hypothesis 4 may involve two competing effects. In our case, with the adhesion having a negative correlation with fiber content, the lower degree of smoothening for high fiber content, and possible better mechanical anchoring, is not a dominating effect compared to other effects in our hypotheses. On the other hand, the smoothening observed for low fiber content may be a sign of softening and interdiffusion.

Regarding hypothesis 5, we can make a rough estimate of the interface temperature by using available data for the thermal effusivities of the bulk materials. At the instance of contact, we can, for example, assume that the

TABLE 4 Thermal effusivities based on data in ref. [42]

Material	Temperature (°C)	Thermal effusivity (J m^{-2} K^{-1} $second^{-0.5}$)
TPE	270	700
PA12	45	803
PA12-GF50	45	907

Abbreviations: PA12, polyamide-12; TPE, thermoplastic elastomer.

hard part and the TPE are at 45°C and 270°C, respectively. If we use the parameters in Table 4, the interface temperatures are estimated to be 149.8°C and 143.0°C, respectively, for PA12 and PA12-GF50. Hence, the interface temperature is roughly 7°C lower for the latter material, and this could contribute to the lower adhesion. Note that the interface temperatures estimated above are far below the melting temperature of PA12 (176°C). In the rough estimate above, we have not considered that PA12 and PA12-GF50 may have different surface temperatures prior to overmolding, due to different thermal properties (conductivity, diffusivity) and therefore different cooling rates for the first shot in the mold prior to overmolding.

However, we observe that the fiber concentration near the surface is lower than in the bulk. Hence, the difference between, for example, PA12 and PA12-GF50, with regard to the interface temperature, will be lower than estimated from the bulk effusivity values. In order to obtain better estimates (than above) of the transient interface temperature for different material pairs, the 2CIM process could be simulated. Furthermore, for a more detailed analysis of the effect of the fiber concentration and orientation near the interface, thermal simulations with discrete glass fibers could be performed. Chen and Wang[43] studied the thermal conductivity of a fiber reinforced thermoplastic, and proposed a model for the anisotropic thermal conductivity, taking into account the fiber fraction, the fiber length/diameter ratio, and the fiber orientations. Chen et al.[44] reviewed key factors affecting the thermal conductivity of polymers and polymer-based composites.

Regarding thermal properties, the glass fiber content may also have indirect effects, for example, via the PA12 crystallinity and orientation. Glass fibers affect the thermal properties of the melt (higher thermal diffusivity and faster cooling), and may therefore affect the crystallinity. A reduction in crystallinity generally reduces the thermal conductivity.[44]

5 | CONCLUSION

The adhesion in 2CIM has been studied, using PA12-GF as the first shot (PA12 with 0, 15, 30 and 50 wt% glass fibers), and TPE as the second shot (a TPV and a TPS, both modified for adhesion to polyamides). This study has focused on the effect of the (nominal) glass fiber fraction on the adhesion (peel force). To the best of the authors' knowledge, very few studies of this kind have been published,[30,31] with limited discussion of the results.

Our main observations are listed below:

- Increased glass fiber fraction gives a reduction in adhesion strength
- Increased melt temperature (of the PA12-GF or the TPE) gives an increase in adhesion strength
- Increased injection rate for the TPE gives an increase in adhesion, but only in a certain range of rates
- The TPS material generally showed higher adhesion strength than the TPV, but both followed the same trends as listed above

Regarding the effect of glass fiber fraction on the adhesion, several hypotheses have been discussed in this article. In the list of hypotheses below, the two first are dismissed as main causes for the glass fiber fraction effect in our study, while the other three seem to be relevant.

- A direct effect of the glass fiber fraction, that is, a reduction in adhesion as more fibers are present at the interface with increasing fiber fraction in the PA12-GF, does not seem to be a major cause, because very few glass fibers are in direct contact with the TPE for any (nominal) fiber fraction.
- An effect of the surface roughness of the PA12-GF before overmolding can be rejected in this study, because the roughness was the same for all fiber fractions.
- The PA12 (polymer) microstructure in the skin of the PA12-GF part could be affected by the fiber fraction. The fiber fraction will affect PA12-GF flow characteristics during injection molding, which in turn may affect the resulting microstructure in the skin, and the fusion between PA12-GF and TPE.
- The "near-surface" thermo-mechanical or rheological properties of the PA12-GF material may have an effect on the fusion mechanism and the resulting adhesion, and the fiber fraction has a large effect on these properties.
- The thermal properties of the PA12-GF part will depend on the glass fiber content, and this may affect the temperature of the PA12-GF at the interface, as the TPE melt contacts the PA12-GF. Based on available thermal data (effusivities), a higher fiber fraction will give a lower interface temperature, and hence, possibly a lower adhesion.

For the three last hypotheses, an important question for further work is how the local "near-surface" properties of the PA12-GF part differ from the bulk properties, and what is the relevant depth of this part (from the surface

and in) which must be considered, in order to analyze the effect of the glass fiber fraction on the adhesion strength.

ACKNOWLEDGMENT

This study is funded by the Research Council of Norway via grants to SINTEF Industry and SFI Manufacturing (grant no. 237900).

ORCID

Anna-Maria M. R. Persson https://orcid.org/0000-0002-9686-5759
Erik Andreassen https://orcid.org/0000-0002-4314-5854

REFERENCES

[1] L.-S. Turng, in *Injection Moulding Handbook* (Eds: T. A. Osswald, L.-S. Turng, P. Graham 2nd Ed.), Carl Hanser, Munich **2008**. Special Injection Molding Processes.
[2] J. G. Drobny, *Handbook of Thermoplastic Elastomers*, 2nd ed., Elsevier, Amsterdam **2014**.
[3] ASDR-399009, *Thermoplastic Elastomers Market - Global Forecast to 2022*, Marketsand Markets, **2017**.
[4] A. K. Bhowmick, H. L. Stephens Eds., *Handbook of Elastomers*, Marcel Dekker, New York **1988**.
[5] *ISO 18064, Thermoplastic Elastomers - Nomenclature and Abbreviated Terms*, International Organization for Standardization, **2014**.
[6] S. S. Banerjee, A. K. Bhowmick, *Rubber Chem. Technol.* **2017**, *90*(1), 1. https://doi.org/10.5254/rct.16.83786.
[7] R. R. Babu, K. Naskar, in *Advanced Rubber Composites* (Ed: G. Heinrich), Springer, Berlin **2010**. https://www.doi.org/10.1007/12_2010_97.
[8] N. Ning, S. Li, H. Wu, H. Tian, P. Yao, G.-H. Hu, M. Tian, L. Zhang, *Prog. Polym. Sci.* **2018**, *79*(10), 61. https://doi.org/10.1016/j.progpolymsci.2017.11.003.
[9] D. J. Buckwalter, J. M. Dennis, T. E. Long, *Prog. Polym. Sci.* **2015**, *45*, 1. https://doi.org/10.1016/j.progpolymsci.2014.11.003.
[10] S. Fakirov Ed., *Transreactions in Condensation Polymers*, Wiley-VCH, Weinheim **1999**. https://doi.org/10.1002/9783527613847.
[11] D. Perrin, R. Léger, B. Otazaghine, P. Ienny, *J. Mater. Sci.* **2017**, *52*(12), 7591. https://doi.org/10.1007/s10853-017-0991-z.
[12] M. Van Duin, M. Aussems, R. J. M. Borggreve, *J. Polym. Sci. Part A Polym. Chem.* **1998**, *36*(1), 179. https://doi.org/10.1002/(SICI)1099-0518(19980115)36:1%3C179::AID-POLA22%3E3.0.CO;2-F.
[13] R. Chandran, C. J. G. Plummer, P. E. Bourban, J. A. E. Månson, *Polym. Eng. Sci.* **2018**, *58*, E82(S1). https://doi.org/10.1002/pen.24662.
[14] K. Bruckmoser, K. Resch, T. Kisslinger, T. Lucyshyn, *Polym. Test.* **2015**, *46*, 122. https://doi.org/10.1016/j.polymertesting.2015.07.004.
[15] A. Islam, H. N. Hansen, M. Bondo, *Int. J. Adv. Manuf. Technol.* **2010**, *50*(1-4), 101. https://doi.org/10.1007/s00170-009-2507-8.
[16] S. Meister, D. Drummer, *Microsyst. Technol.* **2017**, *23*(4), 1017. https://doi.org/10.1007/s00542-016-2820-8.
[17] G. Pompe, M. Bräuer, D. Schweikle, J. Nagel, B. Hupfer, D. Lehmann, *J. Appl. Polym. Sci.* **2006**, *100*(4), 4297. https://doi.org/10.1002/app.23842.
[18] A. Rossa-Sierra, M. Sanchez-Soto, S. Illescas, M. L. Maspoch, *Mater. Des.* **2009**, *30*(10), 397. https://doi.org/10.1016/j.matdes.2009.05.037.
[19] G.-J. Bex, F. Desplentere, J. De Keyzer, A. Van Bael, *Int. J. Adv. Manuf. Technol.* **2017**, *92*(5-8), 2599. https://doi.org/10.1007/s00170-017-0341-y.
[20] M. V. Candal, A. Gordillo, O. O. Santana, J. J. Sanchez, *J. Mater. Sci.* **2008**, *43*(15), 5052. https://doi.org/10.1007/s10853-008-2667-1.
[21] C. Baumgart, D. Weiss, V. Altstädt, *Polym. Eng. Sci.* **2016**, *56*(8), 849. https://doi.org/10.1002/pen.24313.
[22] L. M. Arzondo, N. Pino, J. M. Carella, J. M. Pastor, J. C. Merino, J. Poveda, *Polym. Eng. Sci.* **2004**, *44*(11), 2110. https://doi.org/10.1002/pen.20216.
[23] A. R. Carella, C. Alonso, J. C. Merino, J. M. Pastor, *Polym. Eng. Sci.* **2002**, *42*(11), 2172. https://doi.org/10.1002/pen.11107.
[24] M. Dondero, J. M. Pastor, J. M. Carella, C. J. Perez, *Polym. Eng. Sci.* **2009**, *49*(10), 1886. https://doi.org/10.1002/pen.21415.
[25] S. Nguyen, C. J. Perez, M. Desimone, J. M. Pastor, J. P. Tomba, J. M. Carella, *Int. J. Adhes. Adhes.* **2013**, *46*, 44. https://doi.org/10.1016/j.ijadhadh.2013.05.016.
[26] C. Kuhr, A. Sporrer, V. Altstadt, *AIP Conf. Process.* **2014**, *1593*, 142. https://doi.org/10.1063/1.4873751.
[27] X. Zhang, G. Jiang, H. Wu, S. Guo, *High Perform. Polym.* **2014**, *26*(2), 135. https://doi.org/10.1177/0954008313501531.
[28] *VDI 2019:2016-04, Testing the Adhesion of Thermoplastic Elastomers (TPE) on Substrates*, Beuth Verlag GmbH, Berlin **2016**.
[29] M. Bräuer, B. Hupfer, J. Nagel, D. Lehmann, *Polym. Eng. Sci.* **2002**, *42*(4), 859. https://doi.org/10.1002/pen.10997.
[30] M. Bastian, C. Deubel, M. Leistner, S. Zepnik, *Kautschuk Gummi Kunststoffe* **2017**, *70*, 26. https://www.kgk-rubberpoint.de/en/21152/hardsoft-combinations-based-on-adhesion-modified-tpv-and-polyamide/.
[31] J. Neuer, Plastverarbeiter, **2016**. https://www.plastverarbeiter.de/61523/haftfestigkeit-von-hart-weich-verbunden-optimieren/
[32] S. M. Aharoni, *n-Nylons: Their Synthethis, Structure and Properties*, John Wiley & Sons, Hoboken **1997**.
[33] CAMPUSplastics | Datasheet Grilamid L 20 G. https://www.campusplastics.com/campus/en/datasheet/Grilamid+L+20+G/EMS-GRIVORY/61/a2783d67. (accessed: February 12, 2019).
[34] *ISO 307, Plastics - Polyamides - Determination of Viscosity Number*, International Organization for Standardization, **2019**.
[35] S. B. Munteneau, C. Vasile, *Optoelectron. Adv. Mater.* **2005**, *7*(6), 3135.
[36] S. Todros, C. Venturato, A. N. Natali, G. Pace, V. Di Noto, *J. Polym. Sci. Part B Polym. Phys.* **2014**, *52*(20), 1337. https://doi.org/10.1002/polb.23567.
[37] S. Filippi, H. Yordanov, L. Minkova, G. Polacco, M. Talarico, *Macromol. Mater. Eng.* **2004**, *289*(6), 512. https://doi.org/10.1002/mame.200300334.
[38] M. A. Vargas, N. N. López, M. J. Cruz, F. Calderas, O. Manero, *Rubber Chem. Technol.* **2009**, *82*(2), 244. https://doi.org/10.5254/1.3548248.
[39] J. K. Jørgensen, E. Andreassen, D. Salaberger, *Polym. Compos.* **2019**, *40*(2), 615. https://doi.org/10.1002/pc.24698.
[40] J. P. H. Holmström, *An Experimental and Numerical Study of the Mechanical Behaviour of Short Glass-Fibre Reinforced Thermoplastics*, PhD Thesis, NTNU, Trondheim, **2019**.

[41] N. Billon, J. Giradeau, J. L. Bouvard, G. Robert, *Polymers* **2018**, *10*(10), 1047. https://doi.org/10.3390/polym10101047.
[42] *Moldex3D Database*, CoreTech System Co., Ltd, Hsinchu, Taiwan.
[43] C.-H. Chen, Y.-C. Wang, *Mech. Mater.* **1996**, *23*(3), 217. https://doi.org/10.1016/0167-6636(96)00010-5.
[44] H. Chen, V. V. Ginzburg, J. Yang, Y. Yang, W. Liu, Y. Huang, L. Du, B. Chen, *Prog. Polym. Sci.* **2016**, *59*, 41. https://doi.org/10.1016/j.progpolymsci.2016.03.001.

How to cite this article: Persson AMMR, Hinrichsen EL, Andreassen E. Adhesion between thermoplastic elastomers and polyamide-12 with different glass fiber fractions in two-component injection molding. *Polym Eng Sci*. 2020;60: 1642–1661. https://doi.org/10.1002/pen.25408

THERMOMECHANICAL BEHAVIOUR OF PA12

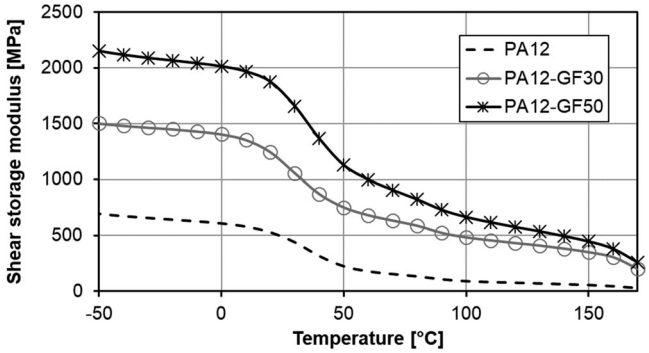

FIGURE A1 Shear storage moduli of PA12 materials (Grilamid L 20 G, Grilamid LV-3, and Grilamid LV-5) vs temperature.[33] PA12, polyamide-12

OPTICAL MICROSCOPY

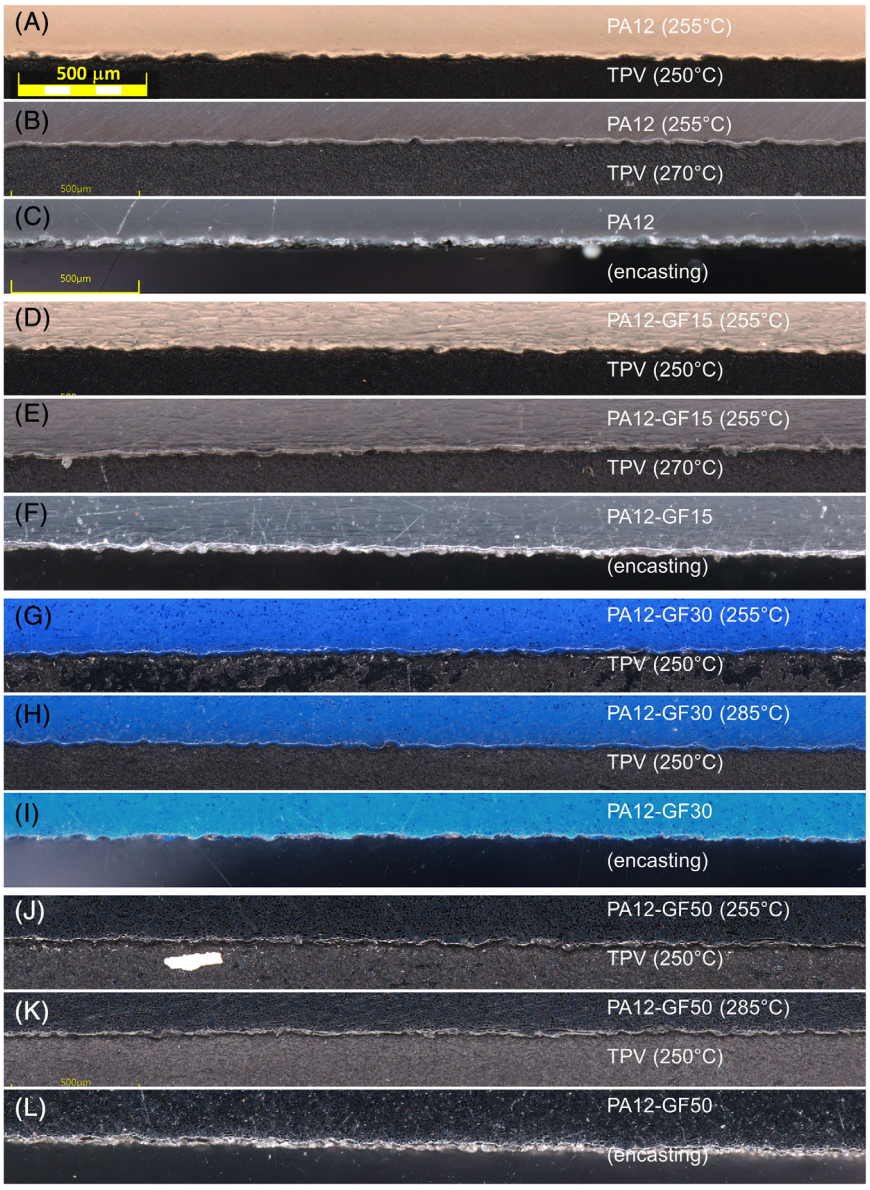

FIGURE B1 Optical microscopy of cross-sections of PA12-GF overmolded with TPV, and (C, F, I, L) without overmolding. The (injection molding) flow direction is into the paper plane, and the cross-section is halfway along the flow path. TPV, vulcanized thermoplastic elastomer [Color figure can be viewed at wileyonlinelibrary.com]

SCANNING ELECTRON MICROSCOPY

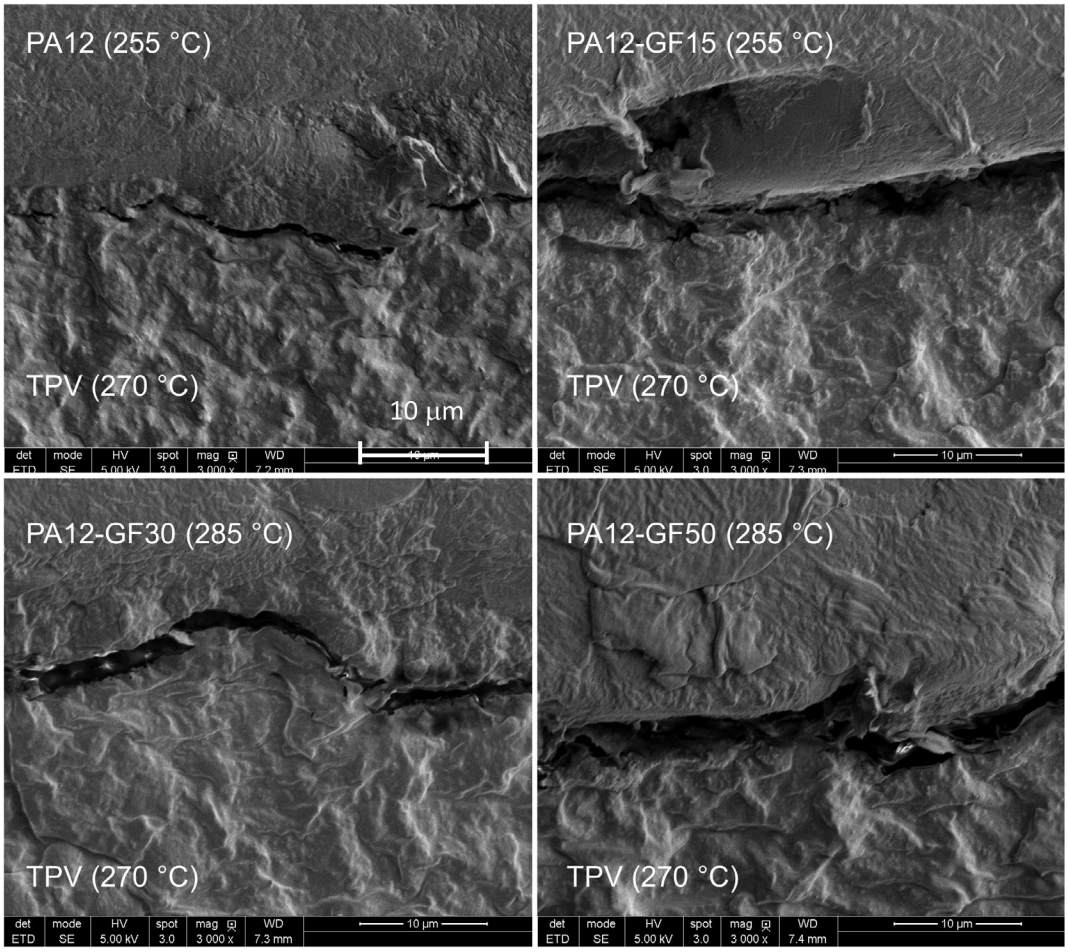

FIGURE C1 High vacuum SEM with high magnification of interfaces PA12 to PA12-GF50 to TPV. PA12, polyamide-12; SEM, scanning electron microscopy; TPV, vulcanized thermoplastic elastomer

WHITE LIGHT INTERFEROMETRY

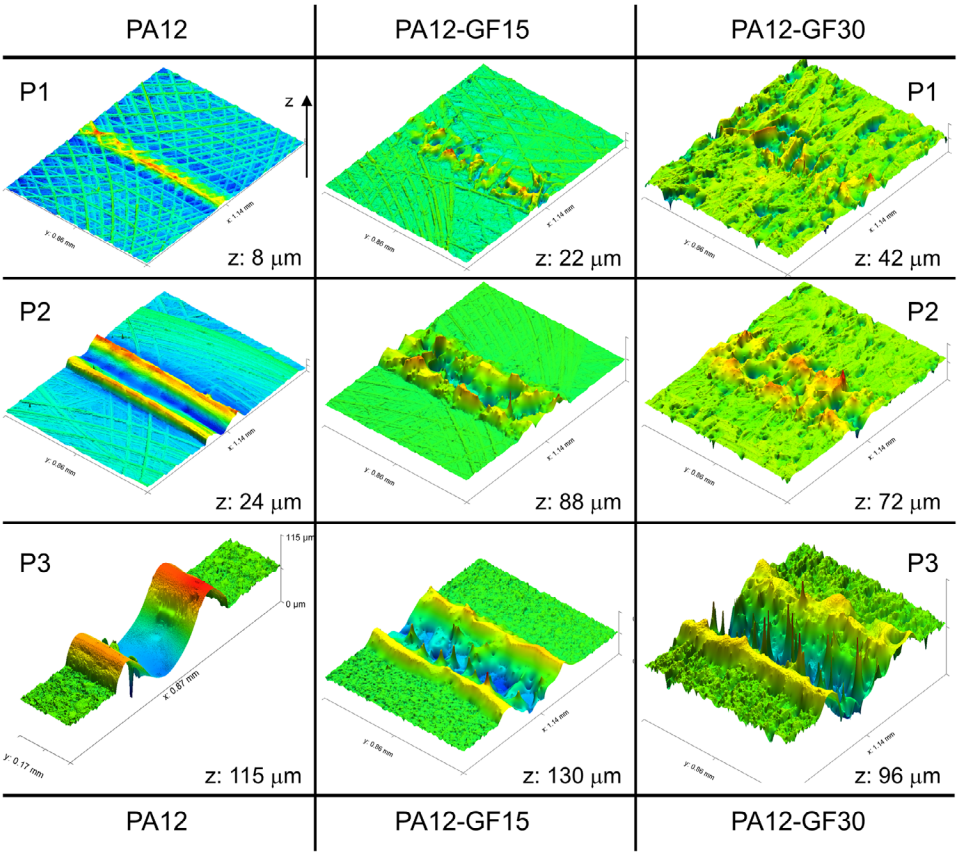

FIGURE D1 WLI measurements of laser engraved PA12-GF substrates. Energy level, substrate, and legend z range are marked in the figure. WLI, white light interferometry [Color figure can be viewed at wileyonlinelibrary.com]

POLARIZED LIGHT MICROSCOPY

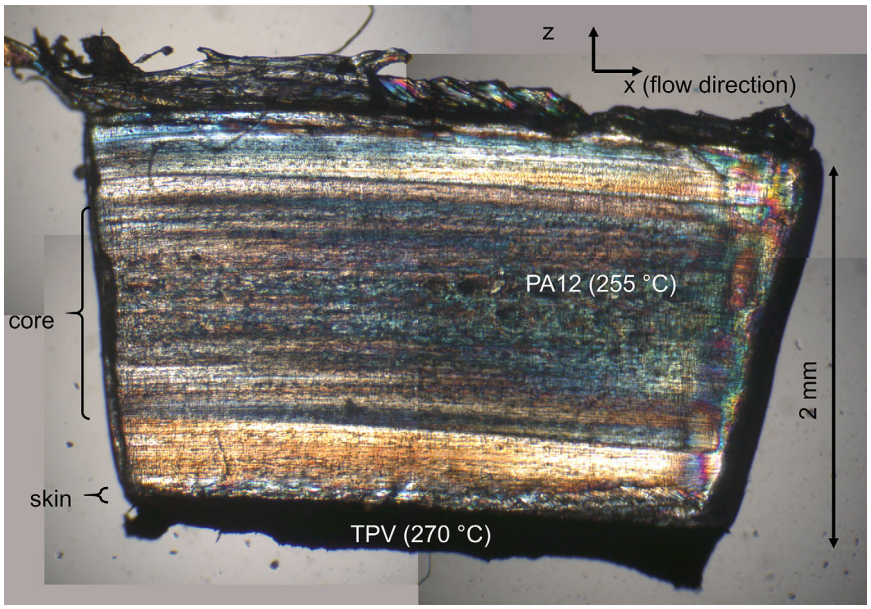

FIGURE E1 Polarized light transmission micrograph (Leica Reichert Polyvar-2, Austria) of a microtome 2CIM TPV on PA12 (TPV part is mostly missing). The core and skin layer from the injection molding are indicated. 2CIM, two-component injection molding; PA12, polyamide-12; TPV, vulcanized thermoplastic elastomer [Color figure can be viewed at wileyonlinelibrary.com]